Tyrosine-Derived Polycarbonate Nerve Guidance Tubes Elicit Pro-Regenerative Extracellular Matrix Deposition When Used to Bridge Segmental Nerve Defects in Swine

Burrell JC[1,2,3], Bhatnagar D[4], Brown DP[1,2], Murthy NS[4], Dutton J[1], Browne KD[1,2], Laimo FA[1,2], Ali Z[1], Rosen JM[5], Kaplan HM[4], Kohn J[4], Cullen DK[1,2,3*]

[1] Center for Brain Injury & Repair, Department of Neurosurgery, Perelman School of Medicine, University of Pennsylvania, Philadelphia, PA

[2] Center for Neurotrauma, Neurodegeneration & Restoration, Corporal Michael J. Crescenz Veterans Affairs Medical Center, Philadelphia, PA

[3] Department of Bioengineering, School of Engineering and Applied Science, University of Pennsylvania, Philadelphia, PA

[4] New Jersey Center for Biomaterials, Rutgers University, New Brunswick, NJ

[5] Dartmouth-Hitchcock Medical Center, Division of Plastic Surgery, Dartmouth College, Lebanon, NH

[*]Corresponding author:

D. Kacy Cullen, Ph.D.
105E Hayden Hall/3320 Smith Walk
Dept. of Neurosurgery
University of Pennsylvania
Philadelphia, PA 19104
Ph: 215-746-8176
Fx: 215-573-3808
Email: dkacy@pennmedicine.upenn.edu

Key Words: Peripheral nerve injury, autograft, tyrosine-derived polycarbonate, nerve guidance tube, extracellular matrix protein deposition, large animal

Abstract

Promising biomaterials for facilitating regeneration should be tested in appropriate large animal models that better recapitulate human inflammatory and regenerative responses than rodent models. Previous studies have shown tyrosine-derived polycarbonates (TyrPC) are versatile biomaterials with a wide range of tissue engineering applications across multiple disciplines. The library of TyrPC has been well studied and consists of thousands of polymer compositions with tunable mechanical characteristics and degradation and resorption rates that are useful for the design of nerve guidance tubes (NGTs). NGTs made of different TyrPCs have been used in segmental nerve defect models in small animals. The current study is an extension of this work and evaluates the effects of NGTs made using two different TyrPC compositions in a porcine model of peripheral nerve injury and repair. We first evaluated a nondegradable TyrPC formulation in a 1 cm segmental nerve defect model in pigs, demonstrating proof-of-concept of chronic regenerative efficacy up to 6 months, at which time nerve/muscle electrophysiology and nerve morphometry were similar to those attained by an autograft repair control. Next, we characterized the acute regenerative response to a degradable TyrPC formulation using the same 1 cm segmental defect model. After 2 weeks *in vivo*, this TyrPC NGT was found to promote the deposition by host cells of pro-regenerative extracellular matrix (ECM) constituents (in particular collagen I, collagen III, collagen IV, laminin and fibronectin) at levels exceeding those deposited inside commercially available collagen-based NGTs. This corresponded with dense and rapid infiltration of host Schwann cells and axons into the lumen of the NGT and axonal crossing of the lesion into the distal nerve segment. These findings confirmed results reported previously in a mouse model and reveal that TyrPC NGTs were well tolerated in swine and facilitated host axon regeneration and Schwann cell infiltration in the acute phase across segmental defects - likely by eliciting a favorable neurotrophic ECM milieu. This regenerative response ultimately can contribute to functional recovery.

Introduction

Peripheral nerve injury (PNI) often results in insufficient functional recovery following surgical repair [1]. Current PNI repair strategies remain inadequate due to inherent regenerative challenges that are dependent on the severity and/or gap-length of the nerve injury. Although small defects can be repaired by suturing the nerve stumps directly together, longer defects require a bridging graft to act as a guide and protective encasement for regenerating axons [2]. Nerve transection results in complete axon degeneration distal to the injury, necessitating axonal regeneration over long distances to reinnervate target end-organs. These long distances are compounded by the relatively slow growth of regenerating axons (~1 mm/day), diminishing the likelihood for significant functional recovery [1].

Nerve autografts are the gold standard for segmental nerve repair. However, various issues have been associated with suboptimal outcomes, including limited availability of donor nerves, donor site morbidity, diameter mismatch, fascicular misalignment, and modality mismatch (sensory nerves are usually used to repair motor/mixed nerve defects) [3]. Despite advancements over the last few decades, there has been limited success in developing a suitable replacement for autografts. Several nerve gap repair solutions are commercially available (e.g., Baxter GEM NeuroTube®, Stryker Neuroflex™, Axogen Avance® acellular nerve allograft), however clinical use remains limited primarily to noncritical sensory nerve injuries, with autografts still being used widely for motor and critical sensory nerve repairs [4]. Thus, there is a clinical unmet need for a technology that at least matches the autograft repair in functional recovery.

Previous reports have demonstrated efficacy of NGTs comprised of degradable polymers in large animal models [5]. More recently, braiding of polymer fibers has been introduced to generate porous NGTs with mechanical properties suitable for nerve repair **[6-8]**. In this study, a braided NGT was fabricated using two polymers chosen from a library of tyrosine-derived polycarbonates (TyrPCs), which have previously been shown to facilitate nerve regeneration in rodent models and demonstrated improved functional recovery in small gap injuries [9-11].

A major consideration for development of novel, clinically translatable NGTs is the inability of rodent models to fully replicate human segemental nerve defects due to critical differences in biological physiology and the short regenerative distances to distal end-target relative to the longer distances implicated in poor functional recovery in humans [12]. Thus, to evaluate whether a novel biomaterial designed for nerve regeneration has potential for clinical translation, proper validation must be performed in a suitable large animal pre-clinical model [13]. The transition of a novel biomaterial from evaluation in a small animal model to a large animal model typically follows a two-step process—the critical first step is to investigate acute regeneration in a short (e.g., 1

cm) nerve gap. At this stage, it is necessary to demonstrate safety and tolerability, ensuring that there is no deleterious inflammatory response, and also efficacy in repairing short gap injuries. The next step is to demonstrate efficacy as a repair strategy for a challenging long gap nerve defect. Here, we report the first phase in the evaluation of braided NGTs for peripheral nerve injury in a 1 cm porcine nerve injury model. In this proof-of-concept, 6-month study in a porcine model, we evaluated functional recovery using a nondegradable TyrPC and compared the pro-regenerative capabilities of degradable TyrPC to commercially-available collagen NGTs at an acute time point. ~~This~~

Methods

TyrPC NGT Fabrication

TyrPC polymers are composed of desaminotyrosyl-tyrosine (DT), desaminotyrosyl-tyrosine ethyl ester (DTE), and different amounts of PEG. TyrPC nomenclature follows the pattern Exxyy (*n*k), where xx and yy are percentage mole fractions of DT and PEG respectively, and *n* is the molecular weight of PEG in kDa [14, 15]. E0000 is a nondegradable homopolymer, poly(DTE carbonate), while E1001(1k) is a degradable terpolymer containing 10% DT and 1% PEG (1 kDa). The main difference between E0000 and E1001(1k) is the rate of degradation: E0000 has a degradation rate of > 6 years *in vivo* and can be regarded as non-degrading over the time course of this 6-month study. E1001(1k) has a degradation rate of 9 to 12 months (depending on implant size and shape) and is significantly degraded over 6 months.

TyrPC polymers were synthesized as described by Magno et al [14]. The fabrication of the TyrPC NGTs is a 3-step process consisting of fiber extrusion, braiding of the NGT, and finally the application of a barrier coating, as described by Bhatnagar et al [11]. The previously published procedure for the fabrication of HA-coated NGTs was followed with some modifications to adjust the NGT diameter to the size required for the swine model [11]. TyrPC polymer powder was melt-extruded into 80–110 μm diameter fibers on a single-screw extruder (Alex James & Associates, Inc., Greenville, SC). The extruded fibers were amorphous, as was the polymer, but the polymer chains were oriented to some degree. The degree of orientation as determined by x-ray diffraction methods was 0.32 on a scale of 0 to 1 [16]. This degree of orientation did not cause any significant shrinkage (reduction in length was less than 1% during the cleaning procedure). These fibers were braided into a tubular NGT (three filaments per yarn; 24 carriers, three twisted fibers/carrier, and traditional 2-over-2 braid) using a tubular braiding machine (ATEX, Technologies Inc., Pinebuff, NC). NGTs were fabricated by braiding the fibers over a 2.3 mm inner diameter Teflon mandrel (Applied Plastics Co., Inc. Norwood, MA) to create NGT walls with a uniform pore size

distribution (65 ± 19 μm). Next, NGTs were sonicated in cyclohexane (1x), followed by 0.5% (v/v) TWEEN 20 in DI water (1x), and a final rinse in DI water (5x), and were then vacuum dried overnight at room temperature. The braided NGTs showed no further shrinkage in length or diameter at 37 °C. The cleaned, dried NGTs were subsequently cut with a thermal cutter to 1.2 cm length and the fibers at either end of the NGT were fused to facilitate suturing during implantation. TyrPC NGTs were then treated under UV light for 45 minutes.

Hyaluronic Acid Hydrogel Coating and Sterilization

The outer surface of the braided NGTs was coated with hyaluronic acid (HA) under aseptic conditions. For this, the TyrPC NGTs were placed on a mandrel and were subsequently dipped in 1% (w/v) sterile thiol-modified cGMP grade hyaluronan solution (cGMP HyStem, ESI BIO, California, USA) for 30 sec. Next, the NGTs were crosslinked in 1% (w/v) cGMP grade poly(ethylene glycol diacrylate) (PEGDA) solution for 30 sec. The coating was air dried 5 minutes. These steps were repeated 20 times resulting in a ~150–200 μm thick HA coating. After the last coating, NGTs were dipped in sterile cGMP grade hyaluronan solution for 30 sec and then dried overnight in a laminar flow hood.

The HA coated braided NGTs (2.3 mm ID, 1.2 cm long) were placed in a sealed aluminum pouch and terminally sterilized by electron beam (E-beam) at a radiation dose of 25 KGy (Johnson & Johnson Sterility Assurance (JJSA), Raritan, NJ). The terminally sterilized cGMP HA coated NGTs were tested for sterility using a TSB test. Upon visual observation of the cGMP HA coated NGTs in the TSB test, no turbidity was observed over the 14 days indicating that the cGMP HA coated NGTs were sterile.

Scanning Electron Microscopy (SEM) Characterization

NGTs were imaged using scanning electron microscopy (SEM, Amray 1830I, 20 kV) after sputter coating with Au/Pd (SCD 004 sputter coater, 30 milliamps for 120 seconds) to assess for any morphological changes.

Operative Technique: 1 cm Segmental Repair of Deep Peroneal Nerve Injury in Swine

All procedures were approved by the University of Pennsylvania's Institutional Animal Care and Use Committee (IACUC) and adhered to the guidelines set forth in the NIH Public Health Service Policy on Humane Care and Use of Laboratory Animals (2015). This study utilized young-adolescent Yorkshire domestic farm pigs, 3-4 months of age weighing 25–30 kg (Animal Biotech Industries, Danboro, PA). A total of 15 pigs were enrolled to (a) evaluate the mechanism of action across the graft zone at 2 weeks post repair (n=13) and (b) compare nerve conduction and muscle electrophysiological functional recovery at 6 months (n=2).

Surgical procedures were performed under general anesthesia. Animals were anesthetized with an intramuscular injection of ketamine (20–30 mg/kg) and midazolam (0.4–0.6 mg/kg) and maintained on 2.0–2.5% inhaled isoflurane/oxygen at 2 L/min. Preoperative glycopyrrolate (0.01–0.02 mg/kg) was administered subcutaneously to control respiratory secretions. All animals were intubated and positioned in left lateral recumbency. An intramuscular injection of meloxicam (0.4 mg/kg) was delivered into the dorsolateral aspect of the gluteal muscle and bupivacaine (1.0–2.0 mg/kg) was administered subcutaneously along the incision site(s) for intra- and post-operative pain management. The surgical site was draped and cleaned under sterile conditions. Heart and respiratory rates, end tidal CO_2, and temperature were continuously monitored in all animals.

A 10 cm longitudinal incision was made on the lateral aspect of the right hind limb from 1.5 cm distal to the stifle joint, and extending to the lateral malleolus as previously described [13]. In brief, the fascial layer was bluntly dissected and the peroneus longus was retracted to expose the distal aspect of the common peroneal nerve diving into the muscle plane between the extensor digitorum longus and tibialis anterior. Further dissection revealed the bifurcation of the common peroneal nerve (CPN) into the deep and superficial peroneal nerves (DPN). A 1 cm defect was created in the deep peroneal nerve, 0.5 cm distal to the bifurcation. The defect was repaired with either: (1) Neuroflex™ NGT (n=4), made from cross-linked bovine collagen (2 mm diameter x 1.2 cm long; Stryker, Mahwah, NJ), (2) E1001(1k) NGT (n=4; 2 mm diameter x 1.2 cm long), or (3) reverse autograft (n=5). For the NGT repairs, the conduit was secured to the nerve stumps using two 8-0 prolene horizontal mattress sutures, 1 mm in from the end, both proximally and distally. For the reverse autograft repair, the 1 cm segment was removed and rotated so that the proximal nerve stump was sutured to the distal autograft segment and the distal nerve stump was sutured to the proximal autograft segment using two 8-0 prolene simple interrupted sutures on each end [3]. The surgical area was irrigated with sterile saline and the fascia and subcutaneous tissues were closed in layers with 3-0 vicryl interrupted sutures. The skin was closed with 2-0 PDS interrupted, buried sutures, and the area was cleaned and covered with triple antibiotic ointment, a wound bandage, and a transparent waterproof dressing.

In a separate experiment, chronic regeneration and recovery was assessed at 6 months following repair of a 1 cm deep peroneal nerve defect with a sural nerve autograft (n=1) or a E0000 NGT (n=1). In this experiment, E0000 was used as this version is non-degradable, which facilitated localization and visualization of the graft zone at 6 months post repair. The sural nerve was selected as the donor nerve for this study as it is considered the “gold-standard” clinical repair strategy for segmental nerve defects. For the sural nerve autograft harvest, a second longitudinal

incision was made approximately 3 cm posterior to the lateral malleolus and parallel to the Achilles tendon. The fascial tissue was dissected to expose the sural nerve running close to the saphenous vein, and a several cm long segment was excised, placed in sterile saline, and then cut into a 1 cm segment for repair of the DPN defect. The deep layers and skin were closed with 3-0 vicryl and 2-0 PDS buried interrupted sutures, respectively.

Muscle Electrophysiological Evaluation

Electrophysiological evaluation was performed at 6 months post repair of the 1 cm deep peroneal nerve defect repaired with either a sural nerve autograft or a E0000 NGT. Here, the DPN was re-exposed under anesthesia, and the segment containing the repair was carefully freed to minimize tension and isolate it from the surrounding tissues. The nerve was stimulated (biphasic; 1 Hz; 0–1 mA; 0.2 ms pulses) 5 mm proximal to the repair zone with a bipolar electrode with bends fashioned to maintain better contact with the nerve (Medtronic, Jacksonville, FL; #8227410). A ground electrode was inserted into subcutaneous tissue halfway between the electrodes (Medtronic; #8227103). Compound muscle action potential (CMAP) recordings were measured with a bipolar subdermal electrode placed distally in the extensor digitorum brevis muscle belly. The stimulus intensity was increased to obtain a supramaximal CMAP and the stimulus frequency was increased to 30 Hz to achieve maximum tetanic contraction. All CMAP recordings were amplified with 100x gain and recorded with 10–10,000 Hz band pass and 60 Hz notch filters.

Compound nerve action potential (CNAP) recordings were measured 5 mm distal to the repair zone with a bipolar electrode as described above. All CNAP recordings were amplified with 1,000x gain and recorded with 10–10,000 Hz band pass and 60 Hz notch filters.

Tissue Processing, Histology, and Microscopy

At the terminal time points, animals were deeply anesthetized and transcardially perfused with heparinized saline followed by 10% neutral-buffered formalin using a peristaltic pump. Hind limbs were removed and post-fixed in formalin at 4 °C overnight to minimize handling artifact. The next day, the ipsilateral and contralateral CPN and DPN were isolated and further post-fixed in 10% neutral-buffered formalin at 4 °C overnight followed by 30% sucrose solution until saturation for cryopreservation. Nerves were embedded in optimal cutting temperature embedding media, flash-frozen, and then sectioned longitudinally (20–25 μm) using a cryostat. After rinsing in 1x phosphate buffered saline, nerve sections were blocked and permeabilized at room temperature using 0.3% Triton-X100 plus 4% normal horse serum for 60 minutes. Primary antibodies diluted in phosphate-buffered saline (PBS) + 4% normal horse serum (NHS) were applied to the sections and allowed to incubate at 4°C for 12 hours. After rinsing in 1x PBS, appropriate fluorescent

secondary antibodies (Alexa-594 and/or -647; 1:500 in 4% NHS solution) were added at 18-24°C for 2 hours. For sections stained with FluoroMyelin (1:500; ThermoFisher Scientific, Waltham, MA), the solution was applied for 20 minutes at room temperature. The sections were then rinsed in 1x PBS and cover-slipped with mounting medium.

All quantitative measurements were made by one or more skilled technicians who were blinded as to the experimental group being evaluated. To assess acute regeneration at two weeks post repair, host regenerating axons were stained with phosphorylated and unphosphorylated anti-neurofilament-H (SMI-31/32 1:1000, Millipore, Burlington, MA; NE1022/NE1023) and Schwann cells were labeled with anti-S100 (1:500; Dako, Carpinteria, CA; Z0311). Axon regeneration and Schwann cell infiltration was measured by evaluating serial longitudinal sections to find the sections with the most deeply penetrating axons and Schwann cells as measured from the proximal stump for axons, and from the proximal and distal stump for the Schwann cells. The mean rate of acute axon regeneration was then calculated by dividing the mean penetration by the number of days *in vivo* (14). The proportion of Schwann cell infiltration was calculated by adding the proximal and distal penetration and dividing by the total gap length (1 cm). Axonal maturation and remyelination was evaluated at 6 months with SMI-31/32 and FluoroMyelin. To evaluate the ECM deposition profiles across the graft region, sections were stained with anti-collagen I (1:500; Abcam, Cambridge, MA; ab34710); anti-collagen III (1:500; Abcam; ab7778); anti-collagen IV (1:500; Abcam; ab6586); anti-laminin (1:500; Abcam; ab11575); and anti-fibronectin (1:500; Abcam; ab6328). The mean intensity and mean intensity relative to the center of the graft was measured for each ECM protein (9-18 regions were sampled per nerve). To determine the mean pixel intensity relative to the center of the graft, regions-of-interest were drawn along the edge (Rw) and center of the NGT (Rm) to calculate the following formula: (Rw-Rm)/Rm. For instance, a mean relative pixel intensity value of 0 would represent a homogenous ECM deposition profile between the edge and center of the graft. A mean relative value of 1 would represent an elevated ECM deposition profile along the edge, whereas a mean relative value of -1 would represent a decreased ECM deposition along the edge. To assess macrophage localization around the graft region at two weeks following repair, sections were stained with anti-IBA1 (1:1000; Fujifilm Wako, Richmond, VA; 019-19741) and Hoechst 33342 (1:10,000; Invitrogen, Waltham, MA; H3570).

Images were obtained with a Nikon A1R confocal microscope (1024x1024 pixels) with a 10x air objective and 60x oil objective using Nikon NIS-Elements AR 3.1.0 (Nikon Instruments, Tokyo, Japan). The mean pixel intensity was measured from images acquired with same confocal settings within regions-of-interest drawn using Nikon NIS-Elements. Mean axon regeneration and

Schwan cell infiltration at two weeks were compared using one-way ANOVA with multiple comparisons (Prism, Graphpad, San Diego, CA). Mean intensity and mean intensity relative to the center of the graft for each ECM protein were compared between collagen NGTs and TyrPC NGTs using one-tailed t-test.

Results

Morphometric and Functional Recovery at 6 Months Post Repair

In the 6-month proof-of-concept experiment, nerve electrical conduction and motor functional recovery was demonstrated at 6 months following a 1 cm segmental nerve repair with E0000 and an autograft. Electrical conduction across the graft and evoked muscle response indicated reinnervation of the neuromuscular junctions at 6 months for both cases and axonal presence, maturation, and remyelination were observed within the graft regions (**Figure 1**). Minimal fibrosis was noted surrounding the repaired nerves, which appeared to be well-vascularized around the graft and more distally. Qualitatively, atrophy of the extensor digitorum brevis muscle appeared consistent between the two animals.

E1001(1k) NGT Fabrication and Hydrogel Coating Characterization

The HA hydrogel uniformally coated the NGTs (**Figure 2)**. E-beam sterilization had no discernible effect on the structure of the NGT or the morphology of HA coating.

Histological Assessment of Nerve Regeneration at Two-Weeks Post Repair

Initial nerve regeneration into the NGTs was evaluated at two weeks post-repair for Collagen or E1001(1k) NGTs. The main bolus of regenerating axons was visualized across the width of the graft zone of the E1001(1k) NGT, collagen NGT, and autograft repairs. The distance this main bolus of axons had grown at two weeks was measured in the graft region for each group, revealing similar axonal penetration of 3.55 mm ± 0.71 mm for the E1001(1k) NGT, 2.82 mm ± 0.73 mm for the collagen NGT, and 4.32 mm ± 1.29 mm for the autografts, thus yielding statistically equivalent rates of axonal regeneration for all test groups ($p=0.24$; **Figure 3**). Substantial Schwann cell infiltration was evident throughout the graft zone of all repaired nerves at two weeks, which was not statistically different between the two NGT groups ($p=0.18$; **Figure 3**).

After two weeks, various ECM proteins were deposited within the graft region of all NGTs. Differences in the ECM deposition profiles between the groups were apparent both qualitatively and quantitatively. The deposition of specific ECM proteins were visualized throughout the lumen of the NGTs, revealing that the presence of collagen III, laminin, and fibronectin was elevated within E1001(1k) NGTs compared to collagen NGTs ($p<0.05$ each). Moreover, when assessing

the ECM deposition at the internal NGT surface (at the biomaterial-cell border) relative to the central lumen, we found that levels of collagen I, collagen III, collagen IV, laminin, and fibronectin were particularly elevated in the E1001(1k) NGTs compared to the collagen NGTs ($p<0.05$ each; **Figure 4**). In the case of the collagen NGTs, ECM deposition for these proteins was concentrated in the center of the NGT, away from the walls as indicated by the negative relative pixel intensity values, whereas in the TyrPC case the ECM deposition was along the walls indicating a potentially broader neurotrophic effect from the material itself. Regenerating axons and infiltrating Schwann cells were found in close proximity to bands of collagen and laminin ECM proteins within the graft zone of both groups (**Figure 5**).

In addition, a moderate level of macrophage activity was found in the graft region in both groups. However, in the case of the collagen NGTs, there was a higher density of activated macrophages along the edge of the NGT compared to a diminished concentration localized around the edge of the E1001(1k) NGTs (**Figure 6)**. This suggests a fundamentally different macrophage response to the E1001(1K) versus collagen NGTs, with the host macrophages working to “wall off” the collagen NGT.

Discussion

Over the last few decades, several NGTs have been developed as an alternative to the autograft repair strategy. Although multiple commercially available NGTs have been approved for clinical application in the United States, autografts remain the gold standard for repairing nerve gaps longer than 3 cm [17]. Recent advancements in bioengineering have allowed for the fabrication of next-generation NGTs with pro-regenerative properties. However, there are several criteria that NGTs must demonstrate prior to clinical deployment. First, NGTs should be porous to allow for waste and nutrient diffusion and exhibit a pore size in the 5–30 μm range to minimize excessive fibrosis and inflammatory cell infiltration [18-20]. The impact of pore size is increasingly important in clinically-relevant long gap nerve injury. In short nerve gap repair, nutrients can reach the center of the graft via longitudinal diffusion from the terminal ends of the conduit. However, in a long gap nerve repair, mass transport of nutrients across the conduit wall is necessary to sustain axon and tissue regeneration along the length of the graft [8, 21]. Next, the conduit must maintain structural support during the early regeneration phase, but then degrade and resorb to decrease any mechanical mismatch with surrounding soft tissue and/or physical impediments to remodeling. The degradation rate should be tailored such that sufficient regeneration occurs prior to loss of tube mechanical properties, or else loss of NGT patency and corresponding graft failure will ensue [22]. NGTs must ultimately degrade into resorbable byproducts, and all materials and

degradation products must be biocompatible, non-cytotoxic, and non-immunogenic. In addition, NGTs should also be flexible and kink-resistant to allow for repair spanning articulating joints. Finally, NGTs must be amenable for suturing to prevent suture pull out and ultimately graft failure.

To comprehensively address these challenges, the Kohn lab previously developed TyrPC NGTs coated with a biocompatible HA-based hydrogel [8, 11]. TyrPCs have previously been shown to be non-toxic and to elicit minimal host responses *in vivo* [14]. HA-coated braided TyrPC NGTs exhibit sufficient porosity for mass transport considerations yet prevent detrimental cellular infiltration into the graft zone [8]. In addition, the specific chemical composition of TyrPC can be tuned, providing a library of otherwise similar polymers with varying degradation and resorption rates. Braided TyrPC NGTs also offer a very high degree of kink-resistance, allowing for over 120° of flexing without luminal occlusion [8]. Earlier small animal studies have demonstrated that TyrPC NGTs significantly enhance regeneration and functional recovery, and exhibit excellent mechanical strength, suturability, and flexibility [8-11]. While new NGT designs are often evaluated in mouse or other rodent models [12], large animal models are uniquely suitable to replicate clinical scenarios and simulate nerve regeneration in humans. Here, we report the next phase in studying braided TyrPC NGTs for nerve regeneration.

In the proof-of-concept chronic porcine study, a 1 cm segmental nerve defect repaired with non-degradable E0000 NGT demonstrated electrophysiological functional recovery at 6 months and showed no signs of excessive inflammatory responses or implant-associated toxicity. Acute regeneration was also studied at two weeks following 1 cm segmental defect repair with degradable E1001(1k) NGTs. E1001(1k) NGTs were compared with commercially-available Stryker Neuroflex NGTs made from crosslinked bovine collagen I. Stryker Neuroflex is a flexible, semipermeable, resorbable tubular matrix with a pore size of 0.1–0.5 μm to enable nutrient transfer [23]. The results showed that E1001(1k) and collagen NGTs supported Schwann cell infiltration and axon regeneration within the lumen yet prevented deleterious fibrotic invasion at two weeks post repair. Although differences between groups were not found to be statistically significant for these metrics, E1001(1k) repairs trended towards improved performance. Interestingly, although similar amounts of ECM proteins were deposited in TyrPC and collagen NGTs, the two groups exhibited stark differences in the distribution of ECM proteins within the NGT. Indeed, collagen I, collagen III, collagen IV, laminin, and fibronectin concentrated along the edge of the TyrPC NGT alone, likely indicating enhanced adsorption to the braided TyrPC fibers as compared to the cross-linked collagen casing. These results are similar to previous findings with E10-0.5(1k) 2D films that have been shown to promote selective adsorption of endogenous ECM proteins laminin, fibronectin, and collagen I, and to promote Schwann cell process spreading

and neurite outgrowth *in vitro* [9]. The early findings suggested that NGTs made from TyrPC may create a "biological niche", or favorable neurotrophic environment, along the inner walls of the NGT that appears to support nerve repair even in the absence of externally added biologics— our current work confirms these findings *in vivo* in a clinically-relevant swine model.

Finally, macrophages play an important role during nerve regeneration by clearing debris and remodeling ECM to facilitates Schwann cell infiltration into the graft region [24]. In this study, macrophages were more concentrated around the edge of the collagen NGT, whereas the distribution of the macrophages appeared more diffuse in the E1001(1k) NGT. The presence of macrophage infiltration along the edges of the NGTs appeared consistent with other studies that have demonstrated NGTs can illicit an immunological response following repair [25]. The implications of these findings and whether there is a relationship with the differences in ECM deposition are currently unclear.

Conclusions

Our data suggests that braided TyrPC NGTs coated with crosslinked HA are biocompatible in large mammals, facilitate nerve regeneration comparable to commercially-available NGTs, and allow nutrient exchange while preventing cellular infiltration. In our 6-month chronic proof-of-concept study, non-degradable E0000 and autograft had qualitatively similar functional recovery. In addition, braided E1001(1k) NGTs demonstrated robust nerve regeneration at two weeks post repair. To our knowledge, these data represent the first report of a fully synthetic NGT that performed similarly and trending towards outperforming a NGT fabricated from collagen, a biologically-sourced material with known neural cell-supportive bioactivity, including promotion of neurite outgrowth. The mechanisms underlying the performance of TyrPCs are likely related to deposition of ECM constituents along the NGT lumen, which could promote infiltration of Schwann cells and engage regenerating axons. These studies broadly suggest that NGTs fabricated from members of the TyrPC library elicit pro-regenerative host responses and promote functional recovery following short-gap nerve injury. Furthermore, synthetic materials, such as TyrPCs, offer advantages over biologics, including reduced batch-to-batch variability and potentially reduced cost following commercial scale-up. Future studies are warranted to thoroughly assess the regenerative efficacy of braided TyrPC NGTs at chronic time points and in longer gap nerve injuries, and to probe potential molecular mechanisms underlying enhanced ECM protein deposition at the material/host interface. In conclusion, TyrPCs are promising materials for fabrication of NGTs with significant translational potential.

Acknowledgements

Financial support was provided by the U.S. Department of Defense [CDMRP/JPC8-CRMRP W81XWH-16-1-0796 (Cullen), MRMC W81XWH-15-1-0466 (Cullen), JWMRP W81XWH-14-1-0100 (Kohn & Cullen), AFIRM W81XWH-08-2-0034 (Kohn & Cullen)]. Additional support was provided by RESBIO - The National Resource for Polymeric Biomaterials funded by the National Institutes of Health (EB001046) (Kohn).

Author Contributions

D.K.C., J.K., and H.K. conceived of and designed experiments. D.B., S.M., H.K., and J.K. designed and carried out TyrPC NGT fabrication and *in vitro* assessment. Z.A., J.R., and H.K., assisted with initial surgical implementation and/or electrophysiological methodology. J.C.B., J.D., and K.D.B. performed nerve repair surgeries and electrophysiology assessments. J.C.B., D.P.B., and F.A.L., performed histological assessment and confocal imaging, and figure preparation. J.C.B. and D.P.B. analyzed data. J.C.B. and D.K.C. conducted initial figure and manuscript preparation. D.K.C. and J.K. oversaw all studies and manuscript preparation. All authors provided edits and comments to the manuscript.

Competing Financial Interests

The authors confirm that there are no known conflicts of interest associated with this publication and there has been no significant financial support for this work that could have influenced its outcome.

Data Availability

The raw/processed data required to reproduce these findings cannot be shared at this time as the data also forms part of an ongoing study. Requests for raw/processed data may be addressed to the corresponding author.

References

[1] T. Gordon, K.M. Chan, O.A. Sulaiman, E. Udina, N. Amirjani, T.M. Brushart, Accelerating axon growth to overcome limitations in functional recovery after peripheral nerve injury, Neurosurgery 65(4 Suppl) (2009) A132-44.
[2] B.J. Pfister, T. Gordon, J.R. Loverde, A.S. Kochar, S.E. Mackinnon, D.K. Cullen, Biomedical engineering strategies for peripheral nerve repair: surgical applications, state of the art, and future challenges, Crit Rev Biomed Eng 39(2) (2011) 81-124.
[3] S.E. Roberts, S. Thibaudeau, J.C. Burrell, E.L. Zager, D.K. Cullen, L.S. Levin, To reverse or not to reverse? A systematic review of autograft polarity on functional outcomes following peripheral nerve repair surgery, Microsurgery 37(2) (2017) 169-174.
[4] D.N. Deal, J.W. Griffin, M.V. Hogan, Nerve conduits for nerve repair or reconstruction, J Am Acad Orthop Surg 20(2) (2012) 63-8.
[5] D. Angius, H. Wang, R.J. Spinner, Y. Gutierrez-Cotto, M.J. Yaszemski, A.J. Windebank, A systematic review of animal models used to study nerve regeneration in tissue-engineered scaffolds, Biomaterials 33(32) (2012) 8034-9.
[6] T. Nakamura, Y. Inada, S. Fukuda, M. Yoshitani, A. Nakada, S. Itoi, S. Kanemaru, K. Endo, Y. Shimizu, Experimental study on the regeneration of peripheral nerve gaps through a polyglycolic acid-collagen (PGA-collagen) tube, Brain Res 1027(1-2) (2004) 18-29.
[7] M. Yoshitani, S. Fukuda, S. Itoi, S. Morino, H. Tao, A. Nakada, Y. Inada, K. Endo, T. Nakamura, Experimental repair of phrenic nerve using a polyglycolic acid and collagen tube, J Thorac Cardiovasc Surg 133(3) (2007) 726-32.
[8] B.A. Clements, J. Bushman, N.S. Murthy, M. Ezra, C.M. Pastore, J. Kohn, Design of barrier coatings on kink-resistant peripheral nerve conduits, J Tissue Eng 7 (2016) 2041731416629471.
[9] M. Ezra, J. Bushman, D. Shreiber, M. Schachner, J. Kohn, Enhanced femoral nerve regeneration after tubulization with a tyrosine-derived polycarbonate terpolymer: effects of protein adsorption and independence of conduit porosity, Tissue Eng Part A 20(3-4) (2014) 518-28.
[10] M. Ezra, J. Bushman, D. Shreiber, M. Schachner, J. Kohn, Porous and Nonporous Nerve Conduits: The Effects of a Hydrogel Luminal Filler With and Without a Neurite-Promoting Moiety, Tissue Eng Part A 22(9-10) (2016) 818-26.
[11] D. Bhatnagar, J.S. Bushman, N.S. Murthy, A. Merolli, H.M. Kaplan, J. Kohn, Fibrin glue as a stabilization strategy in peripheral nerve repair when using porous nerve guidance conduits, J Mater Sci Mater Med 28(5) (2017) 79.
[12] H.M. Kaplan, P. Mishra, J. Kohn, The overwhelming use of rat models in nerve regeneration research may compromise designs of nerve guidance conduits for humans, J Mater Sci Mater Med 26(8) (2015) 226.
[13] J.C. Burrell, K.D. Browne, J.L. Dutton, S. Das, D.P. Brown, F.A. Laimo, S. Roberts, D. Petrov, Z. Ali, J.A. Wolf, D.H. Smith, J. Kohn, J.M. Rosen, H.M. Kaplan, H.I. Chen, D.K. Cullen, A Porcine Model of Peripheral Nerve Injury Enabling Ultra-Long Regenerative Distances: Surgical Approach, Recovery Kinetics, and Clinical Relevance, In Preparation.
[14] M.H.R. Magno, J. Kim, A. Srinivasan, S. McBride, D. Bolikal, A. Darr, J.O. Hollinger, J. Kohn, Synthesis, degradation and biocompatibility of tyrosine-derived polycarbonate scaffolds, Journal of Materials Chemistry 20(40) (2010) 8885-8893.
[15] D. Bhatnagar, K. Dube, V.B. Damodaran, G. Subramanian, K. Aston, F. Halperin, M. Mao, K. Pricer, N.S. Murthy, J. Kohn, Effects of Terminal Sterilization on PEG-Based Bioresorbable Polymers Used in Biomedical Applications, Macromol Mater Eng 301(10) (2016) 1211-1224.
[16] N.S. Murthy, X-ray Diffraction from Polymers, Polymer Morphology2016, pp. 14-36.
[17] S. Kehoe, X.F. Zhang, D. Boyd, FDA approved guidance conduits and wraps for peripheral nerve injury: a review of materials and efficacy, Injury 43(5) (2012) 553-72.

[18] C.B. Jenq, L.L. Jenq, R.E. Coggeshall, Nerve regeneration changes with filters of different pore size, Exp Neurol 97(3) (1987) 662-71.
[19] L.J. Chamberlain, I.V. Yannas, A. Arrizabalaga, H.P. Hsu, T.V. Norregaard, M. Spector, Early peripheral nerve healing in collagen and silicone tube implants: myofibroblasts and the cellular response, Biomaterials 19(15) (1998) 1393-403.
[20] C.L. Vleggeert-Lankamp, G.C. de Ruiter, J.F. Wolfs, A.P. Pego, R.J. van den Berg, H.K. Feirabend, M.J. Malessy, E.A. Lakke, Pores in synthetic nerve conduits are beneficial to regeneration, J Biomed Mater Res A 80(4) (2007) 965-82.
[21] S.H. Oh, J.H. Kim, K.S. Song, B.H. Jeon, J.H. Yoon, T.B. Seo, U. Namgung, I.W. Lee, J.H. Lee, Peripheral nerve regeneration within an asymmetrically porous PLGA/Pluronic F127 nerve guide conduit, Biomaterials 29(11) (2008) 1601-9.
[22] G.C. de Ruiter, M.J. Malessy, M.J. Yaszemski, A.J. Windebank, R.J. Spinner, Designing ideal conduits for peripheral nerve repair, Neurosurgical focus 26(2) (2009).
[23] D. Arslantunali, T. Dursun, D. Yucel, N. Hasirci, V. Hasirci, Peripheral nerve conduits: technology update, Med Devices (Auckl) 7 (2014) 405-24.
[24] A.L. Cattin, J.J. Burden, L. Van Emmenis, F.E. Mackenzie, J.J. Hoving, N. Garcia Calavia, Y. Guo, M. McLaughlin, L.H. Rosenberg, V. Quereda, D. Jamecna, I. Napoli, S. Parrinello, T. Enver, C. Ruhrberg, A.C. Lloyd, Macrophage-Induced Blood Vessels Guide Schwann Cell-Mediated Regeneration of Peripheral Nerves, Cell 162(5) (2015) 1127-39.
[25] G. Keilhoff, F. Stang, G. Wolf, H. Fansa, Bio-compatibility of type I/III collagen matrix for peripheral nerve reconstruction, Biomaterials 24(16) (2003) 2779-87.

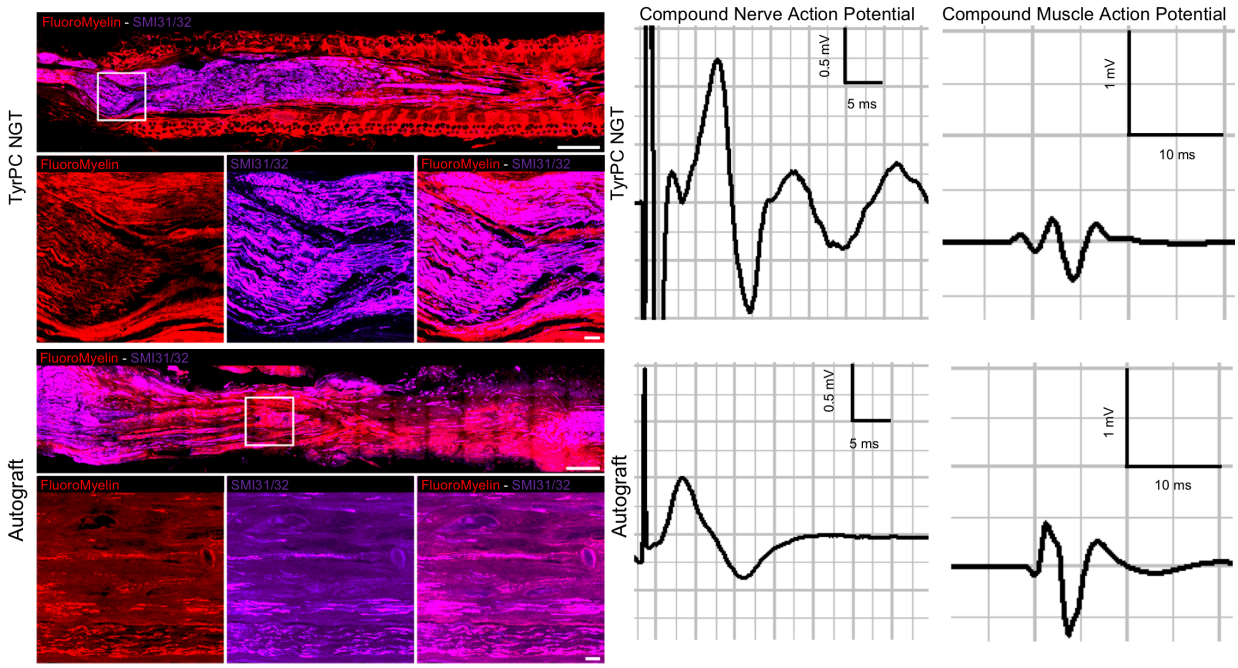

Figure 1. Morphometric and Functional Recovery at 6 Months Post Repair of a 1 cm defect with E0000 NGT and Autograft. Nerve lesions 1 cm in length were repaired with either a reverse autograft or a E0000 NGT (1.2 cm long; HA-coated). Morphometric and functional recovery was assessed at 6 months post repair. Robust axonal regeneration and remyelination were found within both graft regions. Evidence of the TyrPC NGT can be seen in red autofluorescence. Nerve conduction (CNAP) and muscle reinnervation (CMAP) recordings were measured from nerves repaired with either E0000 or autograft repairs. Scale bars: (Top, low magnification) 1000 μm, (Bottom, zoom in) 100 μm.

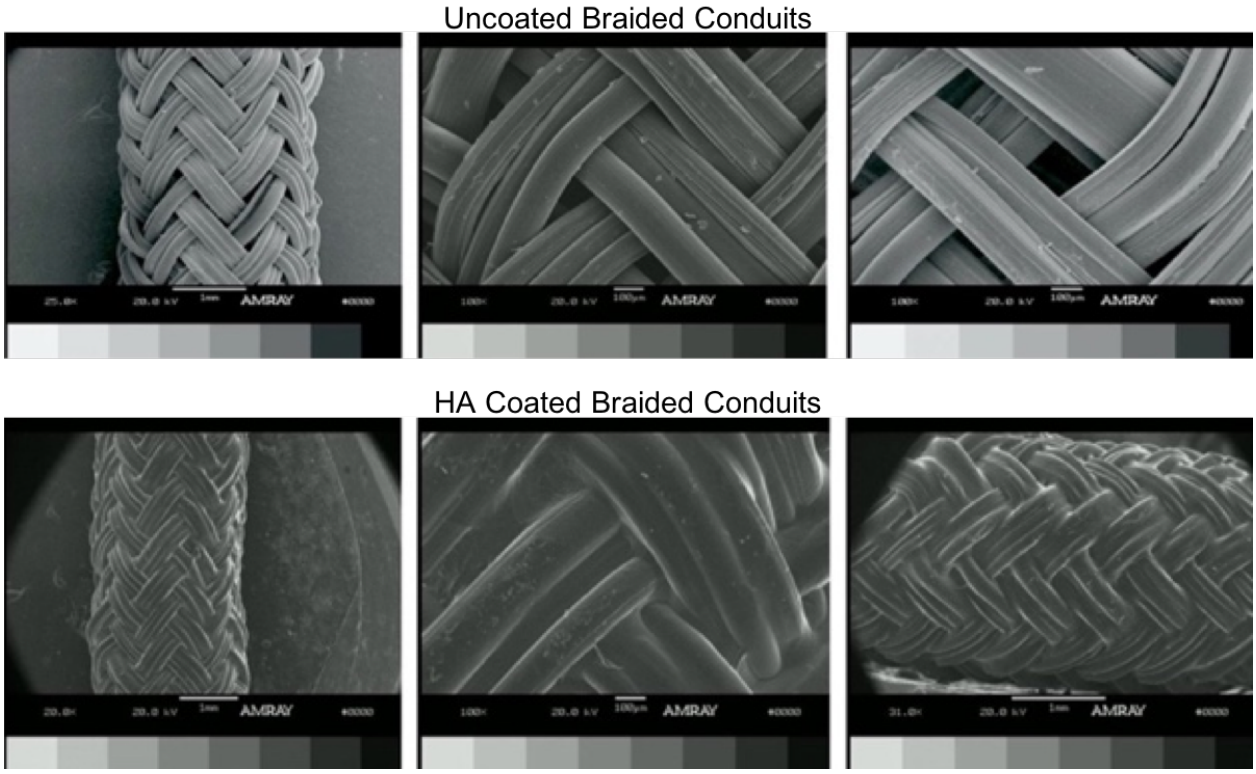

Figure 2. *In Vitro* Characterization of Braided TyrPC NGTs. SEM micrographs of E1001(1k) braided NGTs with triaxial braid shown as uncoated (top) and HA-coated (bottom). The individual fiber diameter varied from 100 μm–200 μm and the average pore size was 90 μm. The HA coating was uniform and covered the pores completely.

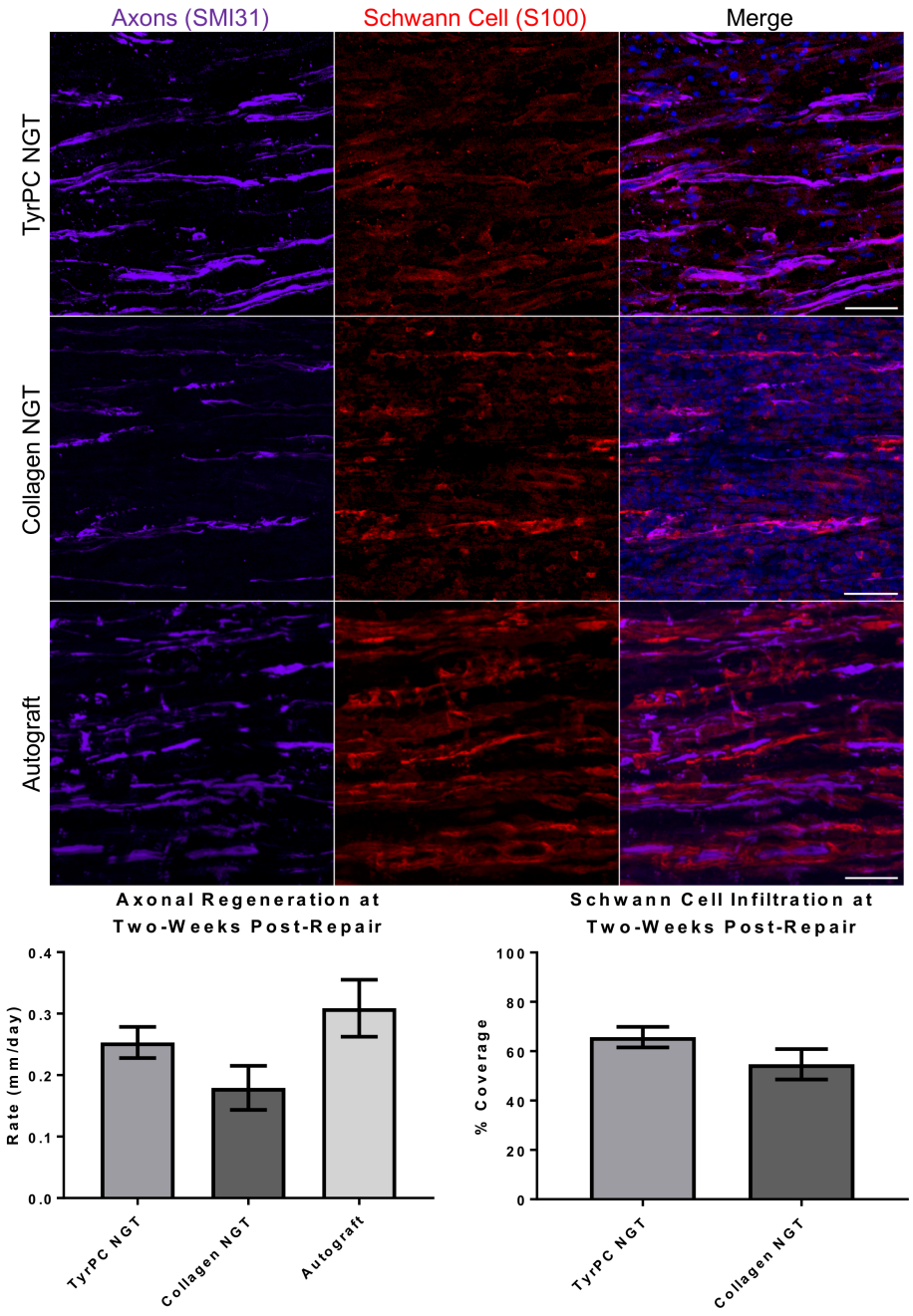

Figure 3. Axon Regeneration and Schwann Cell Infiltration in Nerves Repaired Using Braided E1001(1k) versus Collagen NGTs. At two weeks post repair following a 1 cm nerve lesions, longitudinal sections were stained for axons and Schwann cells. Longitudinal axonal outgrowth was measured and rate was calculated at two weeks post-repair. Schwann cell infiltration was normalized to the entire length of the graft. No significant difference was found between groups for axonal regeneration ($p=0.24$) or Schwann cell infiltration ($p=0.18$). Scale bar: 100 μm.

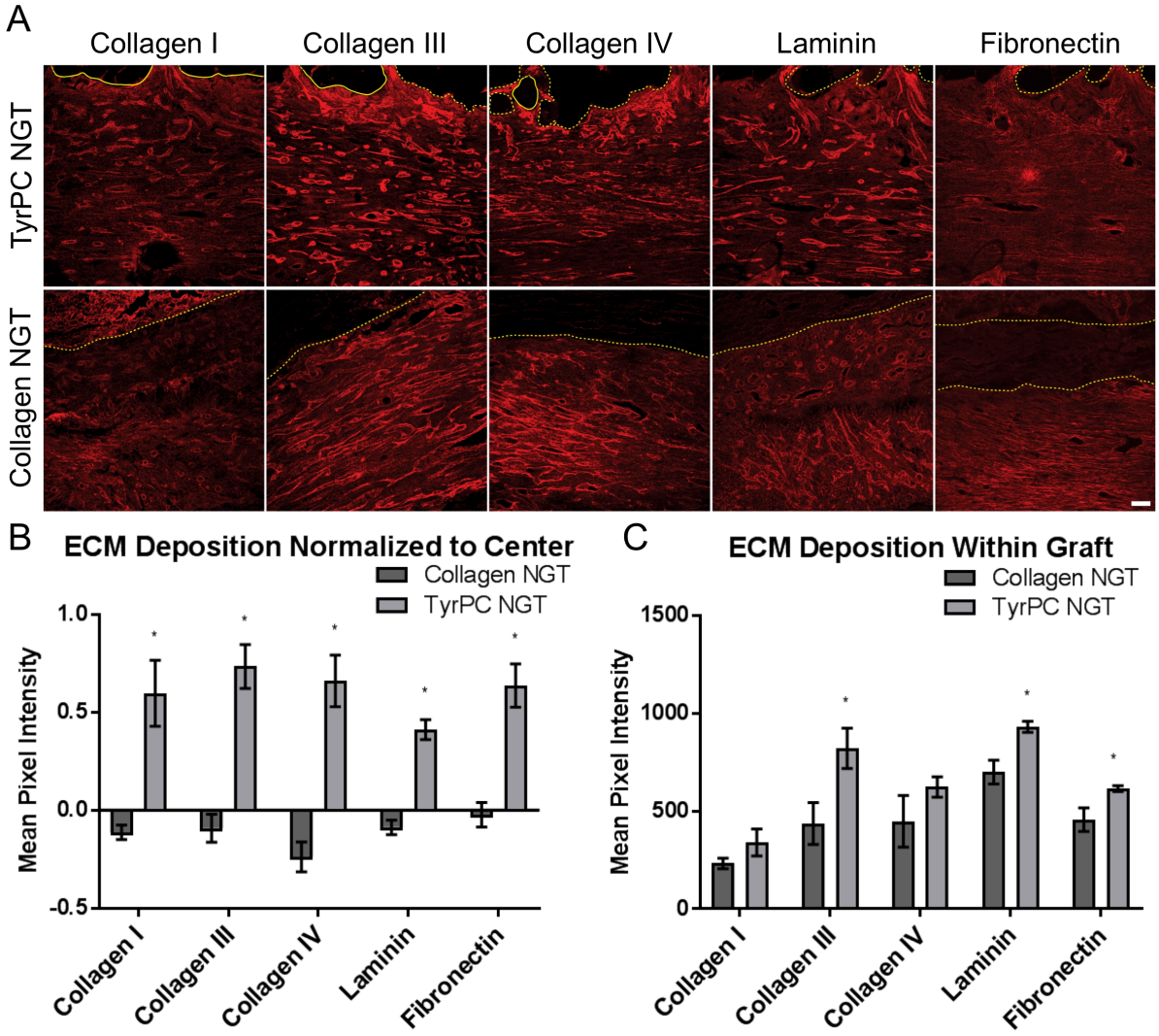

Figure 4. Differential Acute ECM Deposition in Nerves Repaired Using Braided E1001(1k) versus Collagen NGTs. At 2 weeks post repair of 1 cm peroneal nerve lesions, (A) representative longitudinal sections showing deposition of various ECM proteins from animals repaired using braided TyrPC NGTs versus collagen NGTs. Mean pixel intensity are shown for the various ECM proteins relative to (B) the center of the graft and (C) throughout the diameter of the NGT. * $p<0.05$. Scale bar: 100 μm.

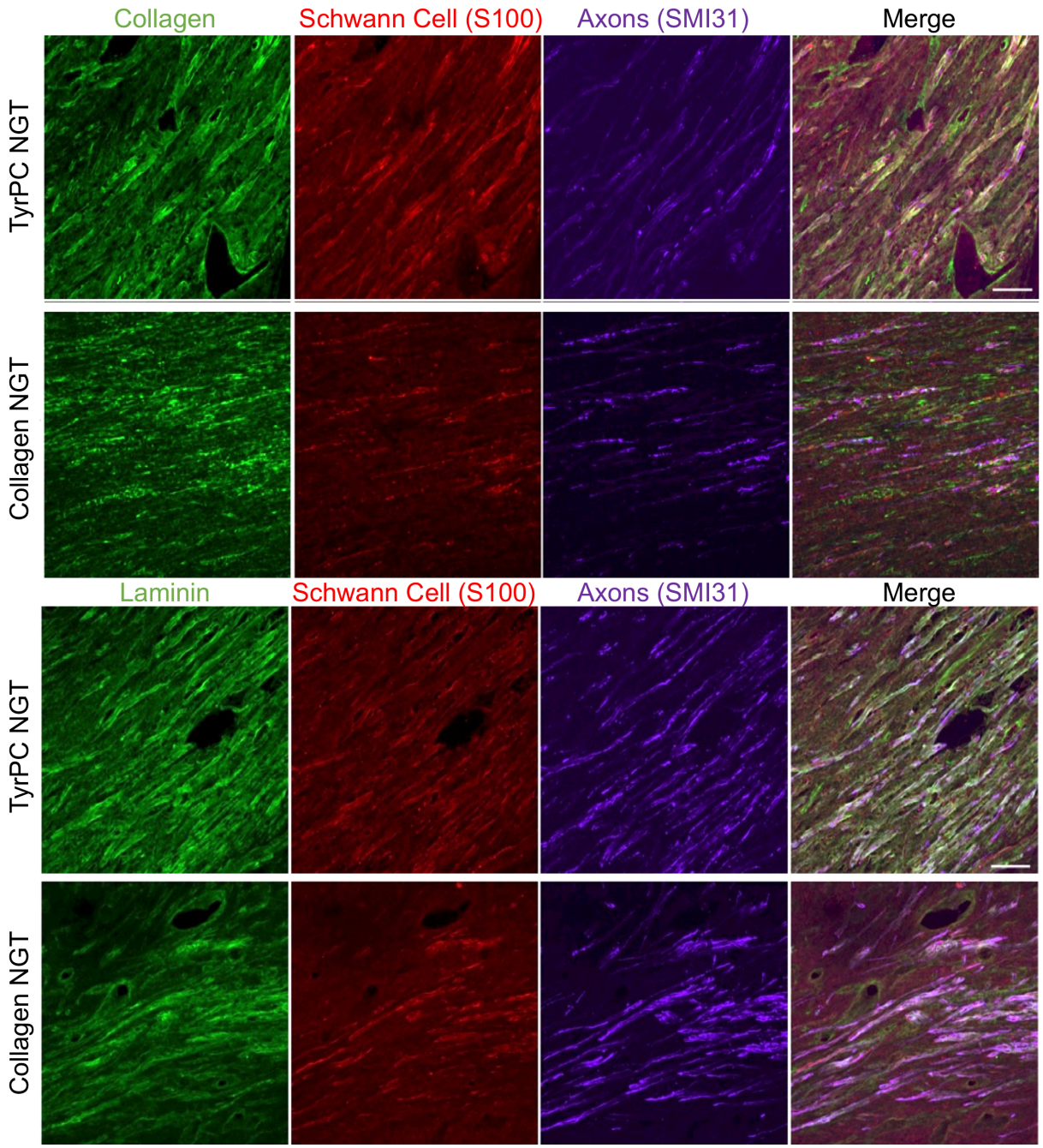

Figure 5. ECM Deposition in Relation to Schwann Cell Infiltration and Axon Regeneration in Nerves Repaired Using Braided E1001(1k) versus Collagen I NGTs. At 2 weeks post repair of 1 cm nerve lesions, representative longitudinal sections showing ECM protein expression and deposition in conjunction with Schwann cell presence and axonal ingrowth. Scale bar: 100 μm.

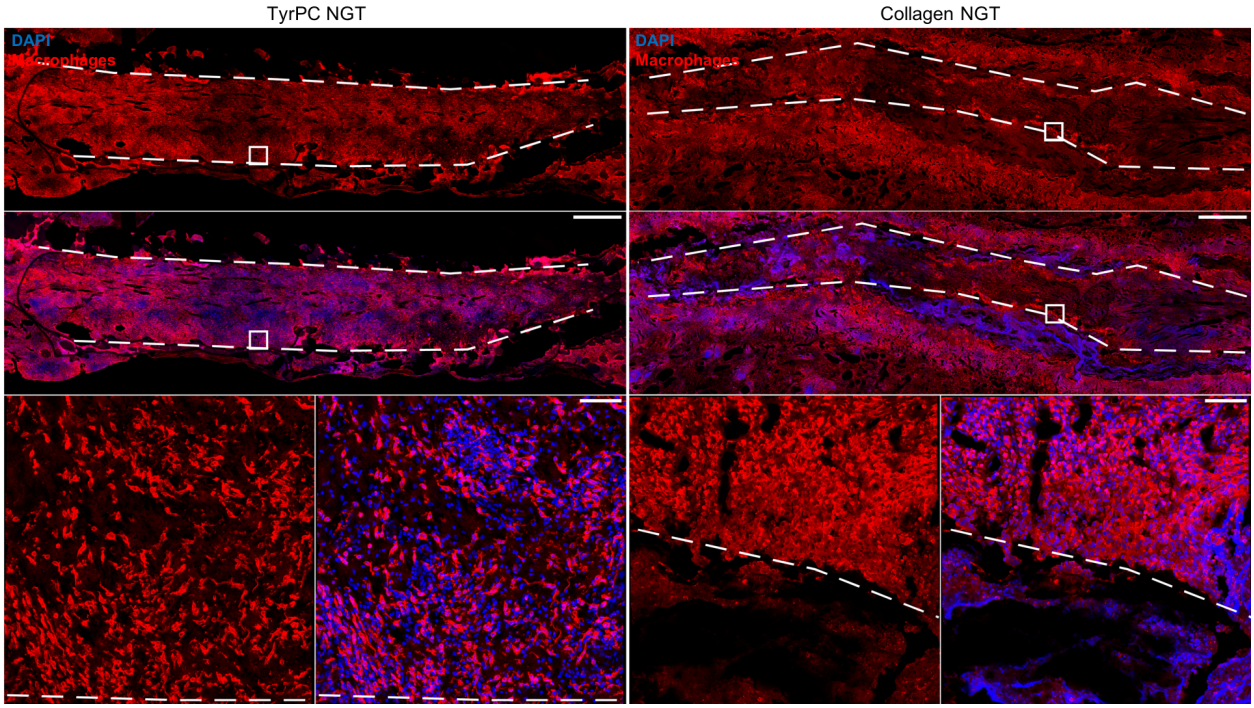

Figure 6. Macrophage Infiltration and Activation Along the Edge of the NGTs Following Nerve Repair Using Braided E1001(1k) versus Collagen NGTs. At two weeks post repair, longitudinal nerve sections were stained for macrophages (IBA1) to evaluate the macrophage reactivity along the NGT. Moderate level macrophage activity was visualized along the edge of the NGT in both groups, with a greater build-up of macrophages at the biomaterial-tissue border for the collagen NGT group. Dashed lines denote the inner edge of the NGT spanning the graft region. Scale bars: (Top, low magnification) 1000 μm, (Bottom, zoom in) 100 μm.